

PARALLEL- AND SERIES-REACTION MECHANISMS OF WOOD AND CHAR COMBUSTION

by

Carmen BRANCA and Colomba Di BLASI

Original scientific paper

UDC: 662.63/.64-942

BIBLID: 0354-9836, 8 (2004), 2, 51-63

Thermogravimetric curves in air of beech wood and char, obtained from conventional pyrolysis of beech wood at a laboratory scale, have been re-examined using different kinetic models. Multi-step reaction mechanisms, consisting of either four (wood) or two (char) reactions are needed for accurate predictions of weight loss curves. In the case of wood, three reactions are linear in the reactant mass fraction whereas the fourth step presents a power-law dependence. A linear reaction for devolatilization and a non-linear reaction for combustion are used for the weight loss curves of char. It has been found that activation energies and pre-exponential factors are invariant with series- or parallel-reactions, providing changes in the stoichiometric coefficients. Furthermore, the activation energies of the two reactions occurring at higher temperatures in the four-step mechanism (wood) and those of the two-step mechanism (char) are the same. Thus, pre-exponential factors and reaction order take into account variations in the char reactivity derived from different pyrolysis conditions.

Key words: *devolatilization, combustion, kinetics, wood, char*

Introduction

The design and optimization of combustors and gasifiers of biomass fuels is based on the knowledge of reaction kinetics. Combustion of biomass consists [1] of pyrolysis, associated with the homogeneous combustion of volatile products, and heterogeneous combustion/gasification of char. Hence information is needed on both the devolatilization stage, that is, about the possible influences of oxygen on the rates of volatile release, and the reactivity of char, whose conversion is 10-100 times slower [2, 3]. However, compared with inert atmospheres, only a few investigations have been carried out on the oxidative decomposition of wood and biomass which, among the most recent, include [4, 5, 6].

Moreover, though the literature on the reactivities of coal chars and their kinetic modeling is huge (see, for instance, the reviews [2, 3, 7]), biomass/wood chars have been examined only in a small number of studies. Most recent publications are [8, 9, 10, 11] and a complete review of previous literature is reported in [11].

Thermogravimetric curves of the decomposition of wood/biomass in the presence of oxygen have been shown to retain, for the low temperature zone, the same qualitative features observed in inert environments [12], followed by combustion of the solid residue.

Consequently, it has been pointed out that a multi-step reaction mechanism is needed, which should at least include a devolatilization and a combustion step. The most recent results [6], obtained with the combined use of integral (TG) and differential (DTG) data, indicate that four reactions are required to take into account the process details. As for char, despite the widely used one-step reaction, DTG measurements also show [10, 11] that combustion is preceded by a devolatilization stage. Hence, a two-step reaction mechanism should at least be used.

This work examines several issues in the kinetic modeling of wood and char combustion not investigated in previous literature. It is not clear whether a parallel- or a series-reaction mechanism should be preferred and how kinetic constants, reaction orders and stoichiometric coefficients vary from one assumption to another. Moreover, the applicability is not known of the kinetics for the char combustion step, as determined from the thermogravimetric analysis of wood, for chars produced from practical systems of biomass pyrolysis.

Experimental

Material

Thermogravimetric tests are re-examined [6, 11] of beech wood (*Fagus sylvatica*) and chars obtained from beech pyrolysis at a laboratory scale. The chemical composition of beech wood [13] comprises 20% lignin, 78% holocellulose and 2% extractives. Chars were produced from pyrolysis of thick (40 mm diameter) wood cylinders radiatively heated along the lateral surface. Results concerning temperature dynamics, conversion times and product yields were already presented elsewhere [13, 14]. Conditions corresponding to an external heat flux of 49 kW/m² with a steady pyrolysis temperature of 800 K and char yields equal to 24% of the initial dry mass of wood are examined here. The elemental analysis of chars produced in this way reports the following contents: carbon 76.4%, hydrogen 3.4%, and nitrogen 0.16%.

Prior to thermogravimetric tests, both wood and char samples were milled to powder (particle sizes below 80 μm) and pre-dried for 10 h at 373 K.

Method

The thermogravimetric system has already been presented elsewhere [15, 16] and only the main characteristics are summarized here. It consists of a furnace, a quartz reactor, a PID controller, a gas feeding system, an acquisition data set, and a precision

balance. The furnace is a radiant chamber, which creates a uniformly heated zone, where a quartz reactor is located.

The sample is exposed to thermal radiation by means of a stainless steel mesh screen, whose sides are wrapped on two stainless steel rods connected to a precision (0.1 mg) balance, which allows the weight of the sample to be continuously recorded. A gas flow (nominal velocity of $0.5 \cdot 10^{-2}$ m/s for the tests discussed in this study) establishes the proper reaction environment and reduces the residence time of vapors inside the reactor.

Solid conversion is made to occur under known thermal conditions by means of feedback control of the sample temperature (measured by a close-coupled thin thermocouple), using the intensity of the applied radiative heat flux as the adjustable variable. The characteristic size of the process is the thickness of the sample layer.

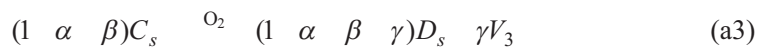
For wood, it was observed that sample thicknesses up to 120 μm allowed a good temperature control, given maximum heating rates of 40 K/min. and a final temperature of 873 K. Also, the weight loss curve was the same as the wood layer thickness was decreased below 120 μm , indicating that spatial temperature gradients were negligible and oxygen diffusion was not the limiting process. Hence, the tests were made for sample layers about 110 μm thick (5 mg distributed over a surface $25 \times 5 \text{ mm}^2$) with heating rates of 5, 10, 20, and 40 K/min for a final temperature of 873 K.

For char, it was observed that sample layer thicknesses up to 120 μm allowed a good temperature control, given maximum heating rates of 15 K/min. and a final temperature of 873 K. Also, the weight loss curve was the same as the char layer thickness was decreased below 120 μm , indicating that a kinetic control was established. Hence, the tests were made for sample layers about 110 μm thick (3.5 mg distributed over a surface $25 \times 5 \text{ mm}^2$) with heating rates of 5, 10, and 15 K/min. for a final temperature of 873 K.

Kinetic mechanisms of wood combustion

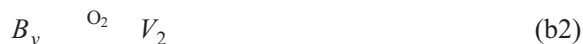
As found in previous studies [6], degradation characteristics of wood in air are qualitatively similar to those already observed in nitrogen. Once devolatilization begins, a more or less pronounced plateau appears, usually associated with hemicellulose degradation. The narrow range of temperatures where cellulose decomposition occurs and the high amounts of volatiles generated are responsible for the attainment of the maximum followed by a rapid decay. A comparison between curves obtained in air and inert atmosphere, for slow heating rates, shows that the hemicellulose shoulder and the cellulose peak are anticipated by about 15 K and 25-35 K, respectively (also, cellulose peaks are about 1.5 times higher). In the absence of oxygen, the peak rate is followed by a wide region of very low values, essentially as a result of lignin decomposition [12]. In the presence of oxygen, given the relatively high temperatures, it is plausible that the activity of the combustion reactions is already important.

Then, combustion leads to the complete conversion of the charred solid. The kinetic models are written using lumped species mass fractions defined in terms of the initial wood mass on ash free basis. The first model is the same proposed by [6] and consists of four series reactions:



where A_s is the virgin solid, B_s , C_s , and D_s charred residues, V_1 , V_2 , V_3 , and V_4 the lumped species representative of volatile species, α , β , γ , and δ the amount of volatile species produced.

The second model consists of four parallel reactions:



where A_v , B_v , C_v , and D_v are the volatile groups, whose initial values are expressed as fractions of the initial wood mass and indicated as α , β , γ , and δ , and V_1 , V_2 , V_3 , and V_4 the lumped volatile species generated.

From the chemical point of view, the first two reactions can be associated mainly with hemicellulose and cellulose degradation, respectively. The third reaction is representative of the final part of the devolatilization process (lignin decomposition) and the beginning of char combustion. The fourth reaction describes char combustion.

The rates of reactions (a1-a3) and (b1-b3) present the usual Arrhenius dependence (A pre-exponential factor and E activation energy) on temperature and are proportional to the mass fractions of reactants (either in the solid or the gas/vapor phase):

$$R_1 = K_1 Y_A, \quad R_2 = K_2 Y_B, \quad R_3 = K_3 Y_C, \quad K_i = A_i e^{-\frac{E_i}{RT}}, \quad i = 1, 3 \quad (1-4)$$

For the char combustion rate, the rate of solid disappearance is generally related to the partial pressure of oxygen through an empirical exponent and the pore surface area available through the reaction volume. Given the relatively high air flow rate employed in the tests, it can be assumed that the oxygen mass fraction remains constant during the reaction process. Consequently, its contribution is incorporated in the pre-exponential factor. Also, a simple power law (n) expression of the solid mass fraction [9] is applied to describe the evolution of the pore surface area during the process:

$$R_4 = K_4 Y_D^n, \quad K_4 = A_4 e^{-\frac{E_4}{RT}} \quad (5)$$

The two models use twelve parameters: the activation energies (E_1, E_2, E_3, E_4), the pre-exponential factors (A_1, A_2, A_3, A_4), the exponent n , and the volatile fractions (indicated in the following as stoichiometric coefficients) (α, β , and γ). The fourth fraction, δ , is obtained from the conservation of the total mass: $\alpha + \beta + \gamma + \delta = 1$.

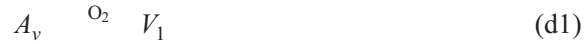
Kinetic mechanisms of char combustion

Thermogravimetric curves of wood char show [11] a low-temperature shoulder followed by a peak which can be associated with devolatilization and combustion, respectively. It has been shown [11] that a two-step reaction mechanism provides accurate descriptions of both integral and differential curves of weight loss. Thus a two-step model is used here, again using lumped species mass fractions defined in relation to the initial char mass on ash free basis. A series-reaction mechanism is considered first:



where A_s is the char, B_s the devolatilized char, V_1 and V_2 lumped species representative of volatile species, ε and ϕ the amounts of volatile species generated.

The second [11] is a parallel-reaction mechanism:



where A_s and B_s are two volatile groups, whose initial values are expressed as fractions of the initial char mass and indicated as ε and ϕ , V_1 and V_2 the lumped volatile species generated.

The rates of reactions (c1, d1) are assumed to present the usual Arrhenius dependence on temperature and to be proportional to the mass fraction of component A_s or A_v :

$$R_1 = A_1 e^{-\frac{E_1}{RT}} Y_A \quad (6)$$

Similar to wood, for the char combustion rate, a power law dependence on the mass fraction of the reactant is assumed:

$$R_2 = A_2 e^{-\frac{E_2}{RT}} Y_B^n \quad (7)$$

The two models use six parameters: the activation energies (E_1, E_2), the pre-exponential factors (A_1, A_2), the exponent n , and the volatile fraction (indicated in the following as stoichiometric coefficient) (ε). The second fraction, ϕ , is obtained from the conservation of the total mass: $\varepsilon + \phi = 1$.

Numerical method

Given the ability to describe both hardwood and softwood decomposition in air for different heating rates, the activation energies, the pre-exponential factors and the exponent n have been taken equal to those estimated in [6] (series reactions) for both models of wood combustion. The same procedure is applied for the kinetic modeling of char combustion. That is, activation energies, pre-exponential factors and exponent n have been taken equal to those estimated in [11] (parallel reactions) for both models of char combustion.

The unknown parameters (stoichiometric coefficients) are estimated through the numerical solution (implicit Euler method) of the mass conservation equations and the associated initial conditions (the temperature is a known function of time) and the application of a direct method for the minimization of the objective functions, which consider both TG and DTG data. The details of the method have been already described by [16].

The fit between measured and calculated curves is defined as:

$$\% \text{dev} = \frac{\sqrt{\frac{S}{N}}}{(\psi_i)_{\text{exp. peak}}} \cdot 100 \quad (8)$$

$$S = \sum [(\psi_i)_{\text{exp}} - (\psi_i)_{\text{sim}}]^2 \quad (9)$$

where i represents the experimental (exp) or the simulated (sim) variable (ψ is the solid mass fraction, Y , or the devolatilization rate, $-dY/dt$) at the time t (N is the number of experimental points and the subscript peak indicates the maximum value).

Results

The results produced by the parallel- and the series-reaction mechanism for wood and char are discussed first. Then, a comparison is made for the two materials examined.

Wood combustion

The results of the kinetic analysis are summarized in tab. 1. Good agreement is obtained between measurements and predictions, as shown in fig. 1 for the solid mass fractions as functions of time and fig. 2 for the devolatilization rates as functions of the temperature. The accuracy of the predictions is slightly higher for the series reactions, as reported by the fit between measured and calculated curves (tab. 1). The ability to take into account the dynamics of different reaction networks by simply varying the stoichiometric coefficients indicate that the differences in the two cases are not exceedingly high.

Table 1. Activation energies, pre-exponential factors, reaction order (n), stoichiometric coefficients and deviations for integral (TG) and differential (DTG) curves for wood (beech) combustion, as estimated by the series- and parallel-reaction models

	E [kJ/mol]				A [s^{-1}]				n
Devolatilization	106				$6.29 \cdot 10^7$				1
	226				$8.60 \cdot 10^{17}$				1
	114				$7.83 \cdot 10^6$				1
Combustion	183				$1.10 \cdot 10^{12}$				1.54
	Series reactions				Parallel reaction				
h [K/min.]	5	10	20	40	5	10	20	40	
α	0.340	0.350	0.420	0.440	0.293	0.320	0.366	0.426	
β	0.415	0.398	0.325	0.304	0.426	0.415	0.358	0.319	
γ	0.115	0.123	0.127	0.158	0.120	0.120	0.120	0.140	
dev _{DTG} [%]	4.6	2.6	6.9	4.0	4.3	3.9	8.4	7.0	
dev _{TG} [%]	1.8	1.4	1.2	1.6	0.4	1.4	0.8	1.0	

The highest amounts of volatiles are always released during the first two reaction stages (devolatilization of hemicellulose and cellulose components). As the heating rate is increased, the volatile amounts released during the first stage become successively higher and those in the second stage lower. Moreover, for the series reaction mechanism, the amounts of volatiles produced from hemicellulose decomposition are slightly higher

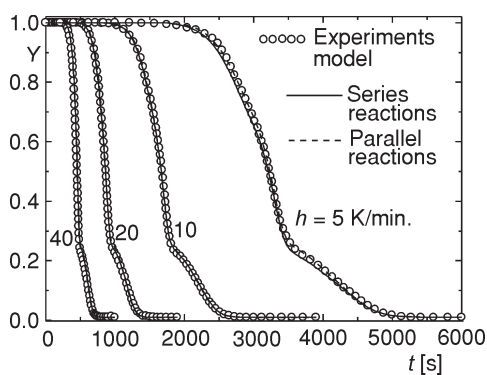


Figure 1. Solid mass fraction for beech wood as measured (symbols) and predicted (lines) for heating rates between 5-40 K/min.

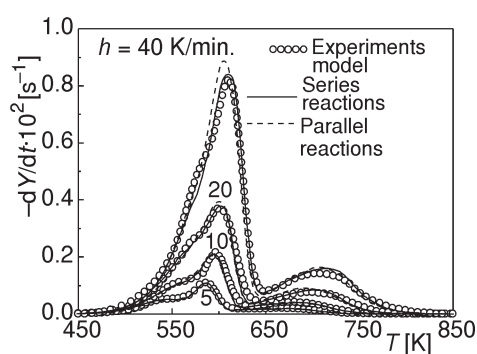


Figure 2. Devolatilization rate for beech wood as measured (symbols) and predicted (lines) for heating rates between 5-40 K/min.

than those generated from cellulose. The contrary occurs for the parallel reaction mechanism. The differences between the other two reaction stages are also relatively small, though the parallel reaction model gives rise to barely higher amounts of char combusted in the fourth step. These results confirm that a large part of volatiles is released at relatively low temperatures (amounts comprised between 72-75%) when heterogeneous reactions are not yet significantly active.

Examples of the time history of the mass fractions and the devolatilization rates of the reactants are shown in figs. 3a and 3b for a heating rate of 5 K/min. and figs. 4a and 4b for a heating rate of 40 K/min. For a meaningful comparison between the mass fractions (figs. 3a, 4a) it should be kept in mind that reactants retain the entire amount of volatiles released in sequence in the series reaction mechanism. On the other hand, in the case of the parallel reaction mechanism, the volatiles are already lumped into four different groups. Therefore, only the A components present dynamics qualitatively similar, though the actual values are highly different in the two cases. The comparison in terms of devolatilization rates (figs. 3b, 4b) is straightforward. A significant overlap, enhanced by high heating rates, between the times of volatile formation exists, independently of the kinetic model. Also, the differences between the two models are small but slightly increasing with the heating rate.

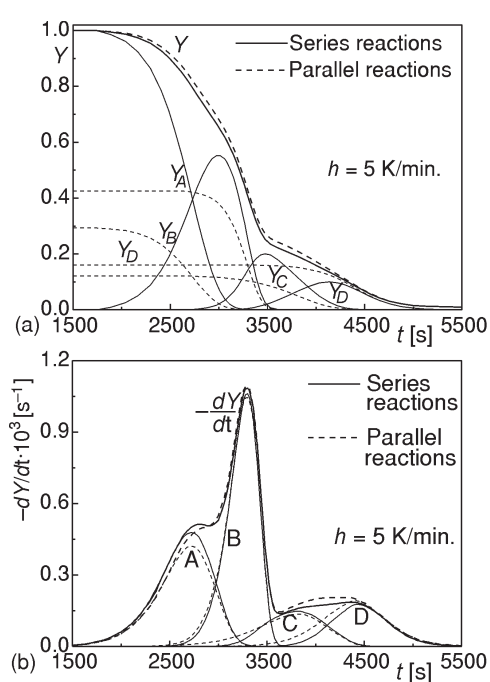


Figure 3. Mass fraction (a) and devolatilization rates (b) of reactants (beech wood) as predicted for a heating rate of 5 K/min.

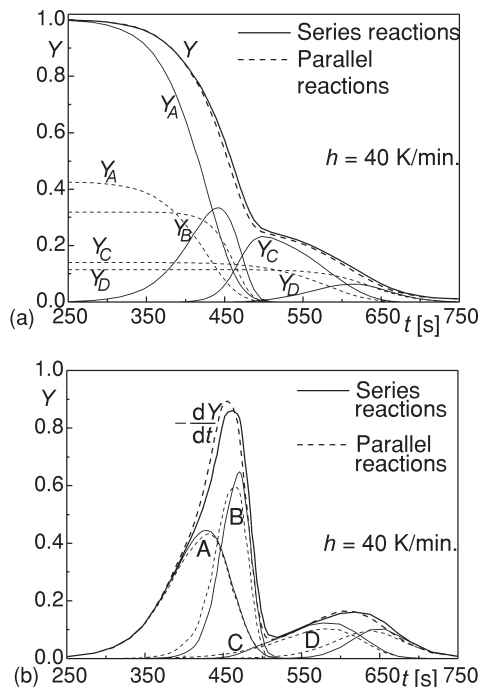


Figure 4. Mass fraction (a) and devolatilization rates (b) of reactants (beech wood) as predicted for a heating rate of 40 K/min.

Char combustion

The results of the kinetic analysis for the weight loss curves of char combustion are summarized in tab. 2 for the two models, whereas figs. 5 and 6 present a comparison between predicted and measured curves (mass fractions and devolatilization rates as functions of time). The agreement between measurements and predictions is very good in all cases, as confirmed by the values of the fit parameters reported in tab. 2. The amounts of volatiles released during the first reaction stage always decrease as the heating rate is increased, but they are slightly lower in the case of parallel reactions. In quantitative

Table 2. Activation energies, pre-exponential factors, reaction order (n), stoichiometric coefficients and deviations for integral (TG) and differential (DTG) curves for char combustion, as estimated by the series- and parallel-reaction models

	E [kJ/mol]		A [s ⁻¹]			n
Devolatilization	114		1.22·10 ⁷			1
Combustion	183		1.40·10 ¹¹			0.90
	Series reactions			Parallel reactions		
h [K/min.]	5	10	15	5	10	15
ε	0.184	0.178	0.176	0.165	0.157	0.155
dev _{DTG} [%]	2.2	5.3	2.0	2.1	5.4	1.9
dev _{TG} [%]	0.9	0.5	0.7	0.7	0.4	0.4

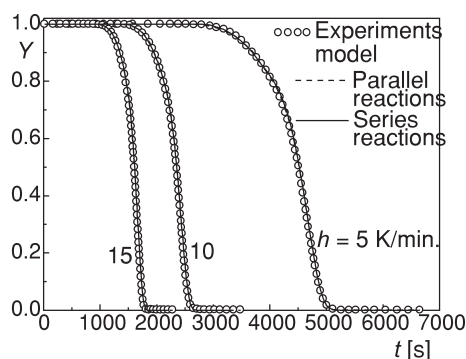


Figure 5. Mass fractions of conventional pyrolysis chars versus time for heating rates of 5-15 K/min. as measured (symbols) and predicted (lines)

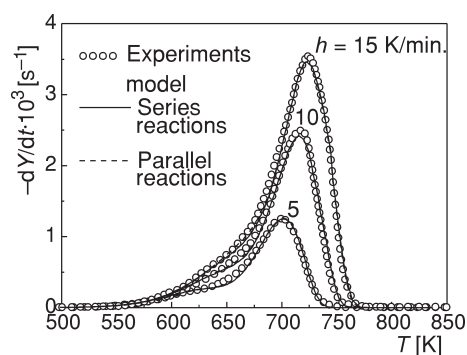


Figure 6. Rates of volatile release from conventional pyrolysis chars versus time for heating rates of 5-15 K/min. as measured (symbols) and predicted (lines)

terms, the effects of the devolatilization reactions are relatively small, as they account only for about 15.5-18.5% of volatiles evolved. This finding motivate the assumption, often made in previous models, of a one-step global reaction for the description of the entire weight loss curve. However, as extensively discussed by [11], the inclusion of a devolatilization step is necessary for a correct evaluation of the kinetic parameters for the second step actually describing the heterogeneous combustion of char. Indeed, the activation energy varies from about 114 (one-step reaction) to 183 kJ/mol (two-step reactions). In this way, in the engineering practice, such data can be safely used.

Examples of the process dynamics for slow (5 K/min.) and fast (15 K/min.) heating rates are shown in figs. 7a and 7b, and figs. 8a and 8b, respectively. Apart from the obvious consideration concerning the different nature of the reactants for the parallel- and series-reaction models, it can be noted that the overlap between the devolatilization and combustion zone is practically unaffected and the change in the heating rate does not play a relevant role in this matter. Compared with wood, the differences between the series- and the parallel-reaction model are even lower.

A comparison can also be made between the kinetic parameters of the two-step mechanisms applied for char combustion (tab. 2) and the last two reactions of the four-step mechanism proposed for wood (tab. 1). The activation energies are the same

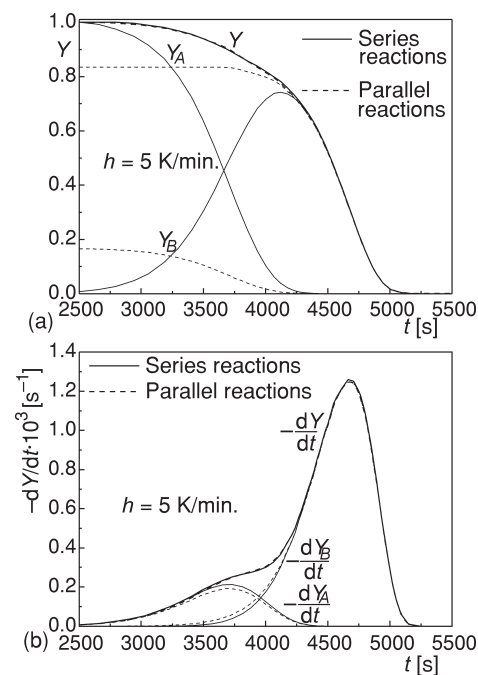


Figure 7. Mass fraction (a) and devolatilization rates (b) of reactants (conventional pyrolysis char) predicted for a heating rate of 5 K/min.

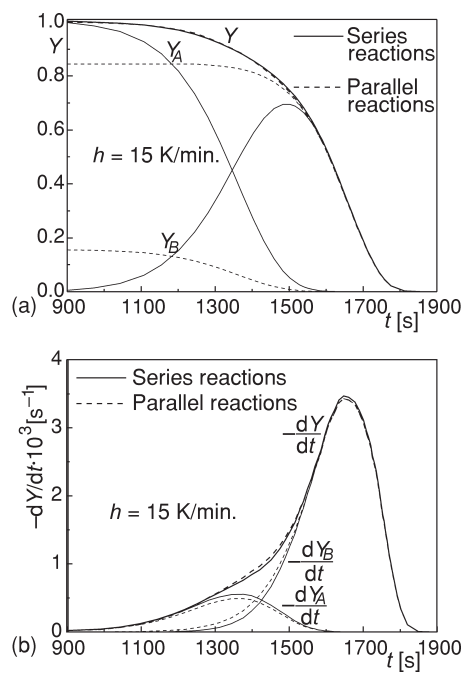


Figure 8. Mass fraction (a) and devolatilization rates (b) of reactants (conventional pyrolysis char) predicted for a heating rate of 15 K/min.

and it can be concluded that the different reactivity of char (caused by different heating rates and temperatures experienced by wood during pyrolysis) can be well described by a simultaneous variation in the exponent n and pre-exponential factors. However, it should also be noted that, for both sets of experiments, the thermal conditions of char formation are those typically encountered in conventional pyrolysis. Therefore further study is needed to determine the modifications in the kinetic parameters needed to describe the behavior of chars generated from fast pyrolysis.

Conclusions

Weight loss curves of beech wood and chars, obtained from conventional pyrolysis of beech wood, have been re-examined to evaluate the applicability of multi-step mechanisms based on either parallel- or series-reaction mechanisms.

A four-step mechanism is shown to describe with a good accuracy the dynamics of the oxidative decomposition of wood. Activation energies, pre-exponential factors and reaction order of the combustion rate for char appear to be invariant with the heating rate and the selection of series or parallel reactions. Moreover, relatively small variations on the stoichiometric coefficients are required to take into account the different structure of the reaction network.

A two-step reaction mechanism describes with a good accuracy the thermogravimetric curves of both mass loss and rate of mass loss in air of conventional pyrolysis chars. Again, activation energies, pre-exponential factors and reaction order do not depend on the heating rate and the application of series or parallel reactions. The variations in the stoichiometric coefficients between the two models are even lower than those computed for wood. Finally, adjustments in the pre-exponential factors and reaction order are sufficient for taking into account the different char reactivities originated from the pyrolysis conditions.

Nomenclature

- A – pre-exponential factor, [s^{-1}]
- A_i – reactant
- B_i – reactant
- C_i – reactant
- D_i – reactant
- E – activation energy, [kJ/mol]
- h – heating rate, [K/min.]
- n – reaction order
- N – number of experimental points
- R_i – rate of reaction
- t – time, [s]
- T – temperature, [K]
- V_i – lumped volatile species
- Y_i – mass fraction of reactant

Greek letters

- α – stoichiometric coefficient
 β – stoichiometric coefficient
 γ – stoichiometric coefficient
 δ – stoichiometric coefficient
 ε – stoichiometric coefficient
 ϕ – stoichiometric coefficient
 ψ – solid mass fraction or devolatilization rate

Subscripts

- DTG – differential curves
 s – solid phase
 TG – integral curves
 v – gas/vapor phase

References

- [1] Kanury, A. M., Combustion Characteristics of Biomass Fuels, *Combustion Sciences and Technology*, 97 (1994), pp. 469-491
- [2] Smith, I. W., The Combustion Rates of Coal Chars: a Review, *Proceedings*, 19th International Symposium on Combustion, Haifa, Israel, The Combustion Institute, Pittsburgh, USA, 1982, pp. 1045-1065
- [3] Ruth, L. A., Energy from Municipal Solid Waste: A Comparison with Coal Combustion Technology, *Progress in Energy and Combustion Science*, 24 (1998), pp. 545-564.
- [4] Bilbao, R., Mastral, J. F., Aldea, M. E., Ceamanos, J., The Influence of the Percentage of Oxygen in the Atmosphere on the Thermal Decomposition of Lignocellulosic Materials, *Journal of Analytical and Applied Pyrolysis*, 42 (1997), pp. 189-202
- [5] Di Blasi C., Branca C., Global Degradation Kinetics of Wood and Agricultural Residues in Air, *The Canadian Journal of Chemistry Engineering*, 77 (1999), pp. 555-561
- [6] Branca, C., Di Blasi, C., Global Intrinsic Kinetics of Wood Oxidation, *Fuel*, 83 (2004), pp. 81-87
- [7] Laurendeau, N. M., Heterogeneous Kinetics of Coal Char Gasification and Combustion, *Progress in Energy and Combustion Science*, 4 (1978), pp. 221-270
- [8] Janse, A. M. C., de Jonge, H. G., Prins, W., van Swaaij, W. P. M., The Combustion Kinetics of Char Obtained by Flash Pyrolysis of Pine Wood, *Industrial and Engineering Chemistry Research*, 37 (1998), pp. 3909-3918
- [9] Di Blasi, C., Buonanno, F., Branca, C., Reactivities of Some Biomass Chars in Air, *Carbon*, 37 (1999), pp. 1227-1238
- [10] Varhegyi, G., Szabo, P., Antal, M. J., Kinetics of Charcoal Devolatilization, *Energy & Fuels*, 16 (2002), pp. 724-731
- [11] Branca, C., Di Blasi, C., Devolatilization and Combustion Kinetics of Wood Chars, *Energy & Fuels*, 17 (2003), pp. 1609-1615
- [12] Gronli, M. G., Varhegyi, G., Di Blasi, C. Thermogravimetric Analysis and Devolatilization Kinetics of Wood, *Industrial and Engineering Chemistry Research*, 41 (2002), pp. 4201-4208
- [13] Di Blasi, C., Branca, C., Santoro, A., Gonzalez Hernandez, E., Pyrolytic Behaviour and Products of Some Wood Varieties, *Combustion and Flame*, 124 (2001), pp. 165-177

- [14] Di Blasi, C., Gonzalez Hernandez, E., Santoro, A., Radiative Pyrolysis of Single Moist Wood Particles, *Industrial and Engineering Chemistry Research*, 39 (2000), pp. 873-882
- [15] Di Blasi, C., Branca, C., Kinetics of Primary Product Formation from Wood Pyrolysis, *Industrial and Engineering Chemistry Research*, 40 (2001), pp. 5547-5556
- [16] Branca, C., Di Blasi, C., Horacek H., Analysis of the Combustion Kinetics and Thermal Behavior of an Intumescent System, *Industrial and Engineering Chemistry Research*, 41 (2002), pp. 2107-2114

Authors' address:

C. Branca, C. Di Blasi
Dipartimento di Ingegneria Chimica,
Università degli Studi di Napoli "Federico II"
P.le V. Tecchio, 80125 Napoli, Italy

Corresponding author (C. Di Blasi)
E-mail: diblas@unina.it
Tel: 39-081-7682232; Fax:39-081-2391800;

Paper submitted: March 23, 2004
Paper revised: April 25, 2004
Paper accepted: April 27, 2004